



													JTT [s]	FT [Hz]	GF [kPa]
P 01	56	M	R	R	0.1	33	1	1	57	27.5	5.4	119.0	30.7	4.8	111.0
P 02	48	M	R	R	251.7	156	2	6	30	35.9	6.7	150.0	120.5	2.3	105.0
P 03	65	M	R	R	0.1	28	1	1	46	36.4	5.5	96.3	64.8	3.3	76.7
P 04	70	M	R	R	3.0	100	3	7	24	47.2	5.6	90.0	158.2	1.5	16.0
P 05	68	M	R	R	40.2	32	3	5	32	39.5	5.4	113.7	165.2	1.7	43.7
P 06	65	M	R	R	1.3	22	2	3	50	47.3	4.5	70.7	68.5	3.5	42.7
P 07	73	M	L	R	0.2	35	1	4	41	37.6	5.3	76.7	69.4	3.9	64.7
P 08	75	M	R	L	0.4	43	1	2	57	26.7	5.3	63.3	27.7	5.1	64.7
P 09	43	F	R	R	42.1	18	2	3	32	33.0	5.4	60.7	144.8	3.0	7.3
P 10	67	M	R	L	1.6	253	1	3	56	32.9	5.1	77.3	34.0	4.2	64.7
P 11	60	M	R	R	2.3	16	1	2	54	43.0	5.7	81.0	46.5	2.9	71.7
P 12	52	F	R	R	26.7	12	1	1	57	28.6	4.6	46.7	38.7	3.7	49.3
P 13	74	F	R	L	0.2	50	1	4	54	33.1	3.3	48.0	41.1	3.1	21.3
P 14	54	M	R	L	10.5	78	2	4	48	32.3	4.5	124.8	88.1	2.1	26.2
Mean	62.1				27.2	62.6	1.6	3.3	45.6	35.8	5.2	87.0	78.4	3.1	54.6
SD	9.8				63.9	65.1	0.7	1.8	11.2	6.4	0.7	29.4	47.3	1.3	30.2
H 01	50	M	R	-	-	-	-	-	-	23.7	6.4	101.7	22.2	5.9	95.0
H 02	66	M	R	-	-	-	-	-	-	28.6	5.8	104.3	28.5	5.5	92.0
H 03	56	F	R	-	-	-	-	-	-	25.9	6.3	48.3	26.9	5.3	40.0
H 04	66	M	L	-	-	-	-	-	-	27.2	5.5	82.3	31.4	5.9	90.0
H 05	61	F	R	-	-	-	-	-	-	32.0	5.6	55.3	33.7	5.1	59.7
H 06	64	M	R	-	-	-	-	-	-	32.5	5.0	102.3	28.3	5.5	119.7
H 07	63	F	R	-	-	-	-	-	-	25.7	5.7	78.0	25.2	6.0	74.0
H 08	56	M	R	-	-	-	-	-	-	26.7	6.4	97.3	26.4	5.7	102.0
H 09	50	F	R	-	-	-	-	-	-	28.6	6.7	62.7	27.2	5.9	66.7
H 10	53	F	R	-	-	-	-	-	-	27.5	5.5	102.7	30.0	4.9	99.7
H 11	55	F	R	-	-	-	-	-	-	25.4	5.5	49.3	29.1	5.1	49.7
H 12	62	M	R	-	-	-	-	-	-	28.6	6.1	107.7	29.8	5.7	112.7
Mean	58.5									27.7	5.9	82.7	28.2	5.5	83.4
SD	5.9									2.6	0.5	23.2	3.0	0.4	25.2

ARAT = Action Research Arm Test; F = female; FT = maximum index finger tapping frequency; GF = maximum grip force; H = healthy control subject; JTT = Jebsen Taylor hand function test; L = left; M = male; m = months; mRS = modified Rankin Scale; NIHSS = National Institutes of Health stroke scale; P = stroke patient; R = right; SD = standard deviation.

cerebral plasticity is high inter-individual variability of the effects induced in both healthy subjects (Daskalakis et al., 2006; Hamada et al., 2013; Muller-Dahlhaus et al., 2008) and stroke patients (Ameli et al., 2009; Grefkes and Fink, 2012). For example, Hamada et al. (2013) demonstrated that application of iTBS in healthy subjects leads to an increase of motor-cortical excitability in only 52% subjects, while the other half responded in an opposite way with a decrease of excitability. Likewise, Ameli et al. (2009) reported that in patients suffering from cortical strokes, only half of them showed behavioral improvements after 10 Hz rTMS while the other half even deteriorated with their stroke affected hands. Such opposed stimulation after-effects are likely to contribute to absent overall effects across the entire group (Hamada et al., 2013).

Apart from known sources of response variability following iTBS like age (Freitas et al., 2011), genetic polymorphisms of the brain-derived neurotrophic factor (Cheeran et al., 2008; Kleim et al., 2006) and technical aspects such as the direction of current flow, the intensity of stimulation and the number of pulses applied (Gamboa et al., 2010; Gentner et al., 2008; Talelli et al., 2007a), clinical factors like lesion location, degree of neurological impairment and time since stroke are also likely to impact on the response to rTMS (Grefkes and Fink, 2012). For example, several studies demonstrated that patients with sub-cortical lesions have a higher probability to improve after rTMS than patients with cortical lesions (Ameli et al., 2009; Hsu et al., 2012). Moreover, the pathomechanisms underlying stroke-induced motor deficits do not only depend on direct tissue damage due to ischemia, but might also comprise network disturbances remote from the stroke lesion (Grefkes and Fink, 2011, 2014). Thus, changes in network interactions are likely to constitute another important factor for the evolution of rTMS-aftereffects as TMS does not only interfere with neural

tissue of the stimulated hemisphere but also with neural activity levels of regions that are interconnected with the stimulation site (Bestmann et al., 2005).

Hence, there is good reason to assume that specific inter-individual differences (or abnormalities post-stroke) in network connectivity might - at least in part - influence response to rTMS. Support for this hypothesis stems from studies with patients suffering from dystonia in which reduced functional connectivity between premotor cortex and M1 was indicative for responding to rTMS (Huang et al., 2010; Quartarone et al., 2003). Furthermore, changes in motor-evoked potential (MEP) amplitudes following rTMS have been shown to be associated with higher effective connectivity between supplementary motor area (SMA), ventral premotor cortex (vPMC) and M1 of the stimulated hemisphere (Cardenas-Morales et al., 2014).

Therefore, in stroke patients, the variability of the individual response to plasticity-inducing intervention might depend on how the stimulation interacts with the pre-existing connectivity in a given functional network, e.g., the motor system. In order to identify factors that are associated with a positive behavioral effect in response to intermittent theta burst stimulation (here: iTBS) applied to ipsilesional M1, we used a multimodal approach consisting of clinical scales, electrophysiological parameters measured using single- and paired-pulse TMS, as well as functional magnetic resonance imaging (fMRI) and dynamic causal modeling (DCM) to assess effective connectivity of the cortical motor network. We reasoned that the systems level perspective offered by DCM might be useful for identifying predictors that indicate whether or not a patient will respond to non-invasive brain stimulation given that (i) focal brain stimulation also impacts on activity levels of areas connected to the stimulation site (Bestmann et al., 2003; Grefkes et al., 2010) and (ii) recovery of motor function depends on changes in

Behavioral and electrophysiological parameters were assessed for each hand/hemisphere before and after each TBS session. The target muscle for MEP recordings was the first dorsal interosseus (FDI). MEP amplitudes of the right and left FDI muscle were measured using Ag/AgCl surface electrodes (Tyco Healthcare, Neustadt, Germany) in a bellytendon montage. The electromyographic (EMG) signal was amplified, filtered (0.5 Hz high pass and 30–300 Hz bandpass), and digitized with a Powerlab 26T device and the LabChart software package version 6.0 (ADInstruments Ltd., Dunedin, New Zealand).

2. Methods

2.1. Subjects

We recruited 14 chronic stroke patients (mean age: 62.8 ± 10.3 years; 10 males) with ischemic lesions (10 right-sided; Suppl. Fig. S1) and 12 healthy controls (58.5 ± 5.9 years; 6 males; Table 1). Inclusion criteria for the patient group were: (i) stable unilateral hand motor deficit, (ii) at least 12 months after stroke (i.e., chronic stage), (iii) absence of aphasia, neglect, and/or apraxia, and (iv) no mirror movements of the unaffected hand during movements of the affected hand (assessed by first interviewing the patient and later by neurological examination and specific motor tests, see below). Three different scales were used to assess clinical impairment of patients: (i) the modified Rankin scale (mRS; rating scale for general disability), (ii) the National Institutes of Health Stroke Scale (NIHSS; rating scale for the presence of neurological symptoms frequently observed in stroke patients), and (iii) the Action Research Arm Test (ARAT; rating scale for hand motor functions like reaching and grasping).

Healthy controls had no history of neurological or psychiatric disease. Please note that the control subjects did not receive iTBS, but rather served as reference for physiological brain activations, brain connectivity and TMS parameters.

One subject in each group was left-handed according to the Edinburgh Handedness Inventory (EHI) (Oldfield, 1971). All remaining subjects were strongly right-handed. EHI was assessed for the time before stroke in patients. None of the subjects had any contraindication to TMS (Wassermann, 1998). All subjects provided informed written consent in accordance with the Declaration of Helsinki (1969, last revision 2008) and approved by the local ethics committee.

2.2. Experimental design

The fMRI experiments were conducted on a separate day before the TBS sessions. Control subjects served as a reference group for TMS parameters and DCM effective connectivity at baseline but did not receive TBS interventions. For the TBS interventions we implemented a sham-controlled within-subject design, in which all patients received two different TBS interventions separated by at least one day to prevent carry-over effects (Fig. 1).

Behavioral and electrophysiological parameters were assessed for each hand/hemisphere before and after each TBS session. The target muscle for MEP recordings was the first dorsal interosseus (FDI). MEP amplitudes of the right and left FDI muscle were measured using Ag/AgCl surface electrodes (Tyco Healthcare, Neustadt, Germany) in a bellytendon montage. The electromyographic (EMG) signal was amplified, filtered (0.5 Hz high pass and 30–300 Hz bandpass), and digitized with a Powerlab 26T device and the LabChart software package version 6.0 (ADInstruments Ltd., Dunedin, New Zealand).

2.3. Theta-burst stimulation (TBS)

Patients received intermittent TBS (iTBS) at the following stimulation sites on two different days: (i) ipsilesional M1 (TMS motor hotspot of the FDI in the stroke-affected hemisphere), and (ii) control stimulation applied to the parieto-occipital vertex (Fig. 1). The iTBS protocol was according to the original publication by Huang et al. (2005). The stimulation order of a given subject (“real-sham” or “sham-real”) was not completely randomized as this could have resulted in a strong

effect. Stimulation was performed using a Magstim Rapid2 stimulator connected to a figure-of-eight TMS coil (Magstim, Whitland, UK). During M1-iTBS, the handle of the TMS coil was pointing posterior and approximately 45° away from the midsagittal line. Hence, the TMS-induced electric current in the brain was approximately perpendicular to the central sulcus, which has been demonstrated to be optimal for excitation of motor neurons (Mills et al., 1992). To reduce possible cortical stimulation effects in the control condition, the coil was held at 45° , touching the skull not with the center but with the rim opposite the handle. In this position, the coil–cortex distance is substantially larger such that the electromagnetic field, if at all reaching the cortex, is substantially weaker and far outside the target (Herwig et al., 2010; Herwig et al., 2007). Of note, we here used a between-subject design of TMS-naïve patients, so there was no prior knowledge that allowed the patients to differentiate between M1- and control-stimulation.

The stimulation intensity was set to 80% active motor threshold (AMT) of the FDI of the stroke-affected hand in both conditions (Huang et al., 2005). Subjects were instructed to avoid any muscle contraction during and up to 5 min after iTBS, which was verified by monitoring EMG activity. In addition to resting and active motor thresholds (Rossini et al., 1994), we used the short-interval intracortical inhibition (SICI) protocol in order to investigate intracortical inhibition within the primary motor cortex prior to rTMS that has been assumed to be mediated by gamma-aminobutyric acid receptor A ($GABA_A$) (Kujirai et al., 1993; Ziemann, 2004). In this protocol, a supra-threshold test stimulus (TS, adjusted to 1 mV) is suppressed if a sub-threshold conditioning stimulus (CS at 80% AMT) is applied 2 ms prior to TS over the same hemisphere. Ten trials with single pulses (TS) and ten trials with paired pulses (CS + TS) were recorded in alternating order.

2.3.1. Behavioral iTBS-effects

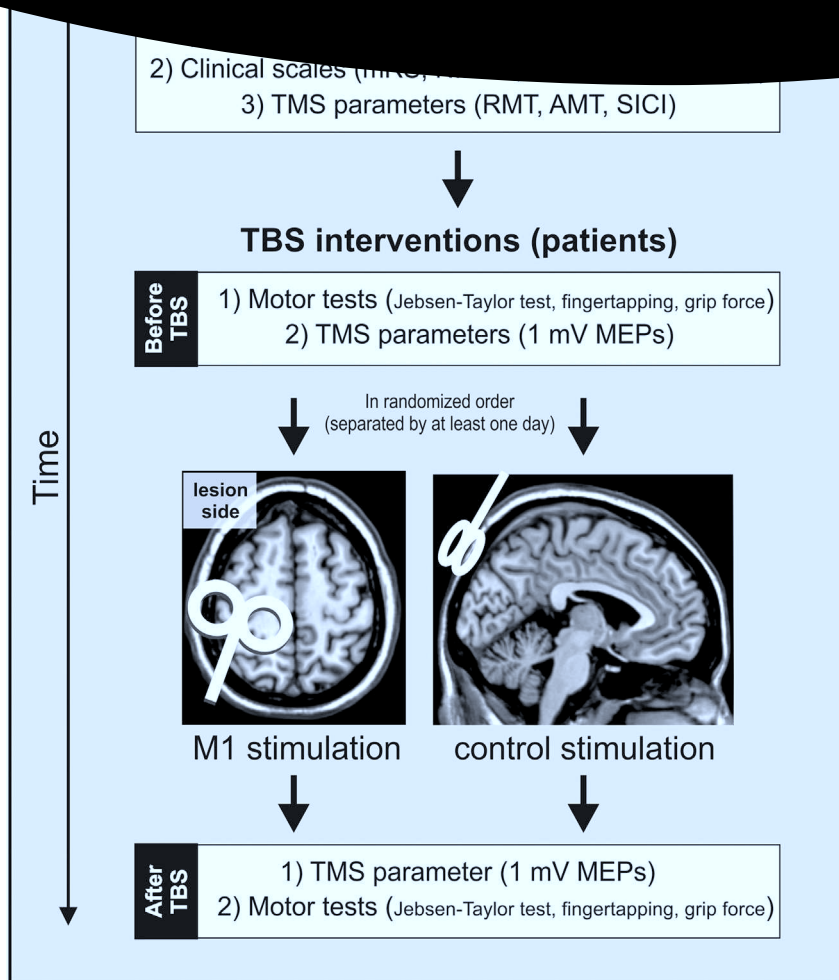
Motor performance of both hands were assessed before and about 15 min after each iTBS session in patients. Three tasks were used to assess different aspects of motor behavior: (i) maximum grip force (GF) measured with a vigorimeter (Martin, Tuttlingen, Germany), (ii) maximum index finger tapping (FT) frequency averaged from five blocks of 5 s, and (iii) the Jebsen Taylor Hand Function Test (JTT) that is a reaction time test for object manipulation of everyday life (Jebsen et al., 1969). The JTT was implemented with all subtests except “writing” as this subtask was too difficult for some of the patients (Celnik et al., 2007; Hummel et al., 2005).

2.3.2. Electrophysiological iTBS-effects

Electrophysiological iTBS-effects were investigated using single-pulse TMS performed with the eXimia NBS system version 3.2.1 (Nexstim, Helsinki, Finland). Stereotaxic frameless neuronavigation ensured that TMS parameters were always obtained from the same position (i.e., the motor hotspot of the FDI muscle). The stimulator output intensity best suited to evoke MEPs with peak-to-peak amplitudes close to 1 mV from the FDI muscle at rest was identified at baseline (SI_{1mV}). Using this stimulator output intensity, fifteen MEPs elicited by single-pulse TMS with an inter-stimulus interval of 7 s were recorded from the contralateral FDI at baseline and about 5 min after iTBS. Analyses of variance (ANOVA) and post-hoc *t*-tests were used to evaluate significant intervention effects.

2.4. Improvement score

To investigate changes in motor performance of the affected hand after iTBS compared to control-TBS composite motor improvement scores were calculated based on changes in GF, FT, and JTT (Rehme et al., 2011b; Ward et al., 2003) based on changes in GF, FT, and JTT as



mRS = modified Rankin Scale; NIHSS = National Institutes of Health Stroke Scale; ARAT = Action Research Arm Test; RMT = resting motor threshold; AMT = active motor threshold; SICI = short-interval intracortical inhibition; MEPs = motor-evoked potentials

described below. The advantage of a composite improvement score is that it is less prone to extreme values or fluctuations in one of the subtests, which is particularly relevant for patients' populations. Furthermore, using one instead of three test-scores prevents the problem of multiple testing. First, changes after each TBS session were expressed in percent relative to the pre-stimulation baseline. Then, changes following control-TBS were subtracted from those following iTBS over M1. Finally, these values were z-standardized and entered as variables into factor analyses with principal component extraction (principal component analysis, PCA, as implemented in SPSS version 21). Thus, the motor improvement score reflected a summary measure of changes in motor performance of the affected or unaffected hand after iTBS compared to control-TBS and baseline. Negative factor values reflect less improvement than the average across the group of patients.

2.5. Functional magnetic resonance imaging (fMRI)

We implemented a block design, in which subjects performed visually paced rhythmic fist closures with their affected or unaffected hand. Fist closures were performed at two different movement frequencies: (i) a fixed frequency of 0.8 Hz and (ii) a frequency individually adjusted to motor performance (40% of the maximum frequency of the respective hand). The fixed frequency condition was

implemented to compare neural activity (between groups or hands) with similar absolute number of movements in one block (resulting, e.g., in similar absolute motor output and re-afferent signals). The adjusted frequency condition was implemented to compare neural activity during movements with similar degree of difficulty. We additionally used the fist-closure frequency of the affected hand as parameter behavioral regressor in the General Linear Model (GLM) to test for correlations between motor performance and connectivity estimates (see below).

The movement frequencies were visually paced by a red blinking circle on a white background presented on a TFT-screen visible via a mirror attached to the MR head coil. Blocks of hand movements (15 s) were separated by resting baselines (13 s plus 0–1.5 s jitter), in which a black screen instructed the subject to rest until instructions were displayed for 1.5 s, indicating which hand to move in the subsequent block. The order of conditions was pseudo-randomized and counter-balanced for each subject. The whole experiment lasted ~18 min. Subjects were trained outside and inside the scanner until they reached stable performance. During the experiment, motor performance was monitored by an MR compatible camera (installed in the scanner room at the foot end of the scanner bed), and analyzed off-line with respect to fist-closure frequencies.

physical T1-weighted images were used to estimate the measured data into un- parameters (time of repetition (TR) = 2070 ms, voxel size = $1 \times 1 \times 1 \text{ mm}^3$). For functional imaging, a gradient-echo planar imaging (EPI) sequence with the following parameters was employed: TR = 2070 ms, TE = 30 ms, voxel size = $3.1 \times 3.1 \times 3.1 \text{ mm}^3$ 31 axial slices. Slices covered the brain from the vertex to lower parts of the cerebellum. Each fMRI session consisted of 537 EPI volumes.

Functional MRI data were analyzed using SPM8. EPIs from patients with a right-sided lesion were mirrored at the midsagittal plane so that for the whole group all lesions were situated within the left hemisphere. To control for hemispheric effects of flipping, EPI volumes of an equal fraction of healthy controls were processed in the same way. “Art.slice” (ArtRepair, <http://cibsr.stanford.edu/tools/human-brain-project/artrepair-software.html>) was used to detect and repair “outlier” slices resulting, e.g. from excessive head movements. The software default threshold was applied to all subjects and resulted in well-tolerable 6.1% of slices being repaired. After spatial realignment, “art.global” was additionally used to detect outlier volumes that either differed considerably in global intensity (i.e., variation in global intensity > 1.3%) or exhibited high scan-to-scan head motion (> 0.5 mm/TR). The outlier volumes were repaired by interpolation between the nearest intact (i.e., non-repaired) scans.

After realignment of the EPI volumes, all volumes were spatially normalized to the standard template of the Montreal Neurological Institute employing the unified segmentation approach (Ashburner and Friston, 2005). Individual lesion masks (based on the lesion extent derived from the T1 scans) were used as cost function during segmentation, and the resulting deformation parameters were applied to the individual EPI volumes. Finally, data were smoothed using an isotropic Gaussian kernel of 8 mm full-width-at-half-maximum (FWHM).

For the first-level analysis, boxcar vectors of each condition were convolved with the canonical hemodynamic response function as implemented in SPM8 in the framework of a general linear model (GLM). The head movement parameters as estimated by the realignment procedure were used as nuisance regressors in the design matrix.

2.7. Voxel-based lesion symptom mapping (VLSM)

To determine whether iTBS-effects detected at the behavioral level depended on lesion location, we performed a voxel-based lesion-symptom mapping (VLSM) analysis with MRICron (Bates et al., 2003). Lesion masks were interactively constructed based on the T1 image of each patient, and then subsequently normalized to MNI. A non-parametric Lieberman quasi-exact test was used to identify those voxels that differentiated between patients showing a positive response following iTBS (according to the improvement score) compared to those with less or missing response.

In stroke patients suffering from motor deficits, the integrity of the corticospinal tract (CST) is an important predictor for recovery (Stinear et al., 2012). To assess whether also the iTBS response is related to the integrity of the CST, the degree of CST damage was estimated based on probabilistic myeloarchitectonic maps (Burgel et al., 1999). Accordingly, individual lesion masks were superimposed upon the probability map data as implemented in the SPM Anatomy Toolbox (Eickhoff et al., 2005). CST damage was defined as intersection volume of individual lesions relative to the total CST volume (Rehme et al., 2015; Volz et al., 2015). These intersection volumes were then correlated with individual iTBS responses using VLSM as implemented in MRICron.

2.8. Dynamic causal modeling (DCM)

We used deterministic bilinear DCM8 (Friston et al., 2003) as

physically valid model to describe the measured data into un- parameters (time of repetition (TR) = 2070 ms, voxel size = $1 \times 1 \times 1 \text{ mm}^3$). For functional imaging, a gradient-echo planar imaging (EPI) sequence with the following parameters was employed: TR = 2070 ms, TE = 30 ms, voxel size = $3.1 \times 3.1 \times 3.1 \text{ mm}^3$ 31 axial slices. Slices covered the brain from the vertex to lower parts of the cerebellum. Each fMRI session consisted of 537 EPI volumes.

As DCMs are computed on the single subject level, we extracted the first eigen variate of the fMRI time-series, adjusted for effects of no interest, from 8 regions-of-interest (ROIs) with 4 mm radius were defined at subject's specific coordinates of activation maxima based on individually normalized SPMs. The ROIs consisted of M1, SMA and vPMC, representing core regions of the motor system and were extracted from respective SPM-T-contrast images in each subject from both hemispheres using a threshold of $P < 0.001$ (uncorrected) (Witt et al., 2008). We chose vPMC rather than dPMC as vPMC neurons are especially engaged in grasping hand movements, while dPMC neurons are predominantly engaged in arm/reaching movements (Grefkes and Fink, 2005; Rizzolatti and Luppino, 2001). The preference of vPMC for hand motor function was also reflected by the fMRI data of the present study that clearly showed a separable vPMC cluster while dPMC was only weakly activated, and the area of activation extended typically into the M1 activation cluster (Fig. 4). Based on structural connectivity data derived from invasive studies in macaque monkeys (Boussaoud et al., 2005; Luppino et al., 1993; McGuire et al., 1991; Rouiller et al., 1994), we assumed endogenous connections (DCM-A-matrix). As hand movements were triggered by a blinking visual cue, we assumed that activity in premotor areas (SMA, vPMC) was driven by visual cortex activity (V1) (Fig. 4). Therefore, we included V1 as the input regions modeled in the DCM-C-matrix (Eickhoff et al., 2008; Grefkes et al., 2008a; Rehme et al., 2013; Rehme et al., 2011a). Please note that none of the lesions in the patient group affected any of the ROIs.

2.8.1. Bayesian model selection

We assumed that all motor ROIs are intrinsically connected with each other (DCM-A-matrix) based on findings of invasive tract tracing studies obtained in macaque monkeys (McGuire et al., 1991; Rouiller et al., 1994). Based on the DCM-A-matrix, we set up 36 alternative models of varying complexity reflecting biologically plausible hypotheses on interregional coupling. The first model (model 1) assumed that all possible connections were modulated by the hand motor task (“fully connected model”). Based on this model with 30 connections, connectivity was systematically varied by omitting one (model 2–5, Suppl. Fig. S2A), two (model 6–11, Suppl. Fig. S2B), three (model 12–15, Suppl. Fig. S2C) or four interhemispheric connections (model 16, Suppl. Fig. S2D). All models assuming asymmetric interregional coupling were mirrored at the midsagittal plane (model 17–18, Suppl. Fig. S2E; model 19–23, Suppl. Fig. S2F; model 24–27, Suppl. Fig. S2G; model 28, Suppl. Fig. S2H) if the mirrored counterpart was not already tested. Finally, a less complex model assuming only reciprocal intrahemispheric connections between all three regions and interhemispheric connections between homologous regions was tested (model 29, Suppl. Fig. S2I) and modified by omitting one (model 30–32; Suppl. Fig. S2J), two (model 33–35, Suppl. Fig. S2K) or all three (model 36, Suppl. Fig. S2L) interhemispheric connections. For all models, V1 served as sensory input region (DCM-C) onto all premotor areas (i.e. SMA and vPMC bilaterally) as movements were driven by a blinking visual cue. We then used random-effects Bayesian model selection (BMS) to identify the model with highest evidence given the data (Stephan et al., 2009).

2.8.2. Statistical analysis of DCM coupling parameters

The statistical significance of the coupling parameters of the model with highest expected probability was tested by means of one-sample,

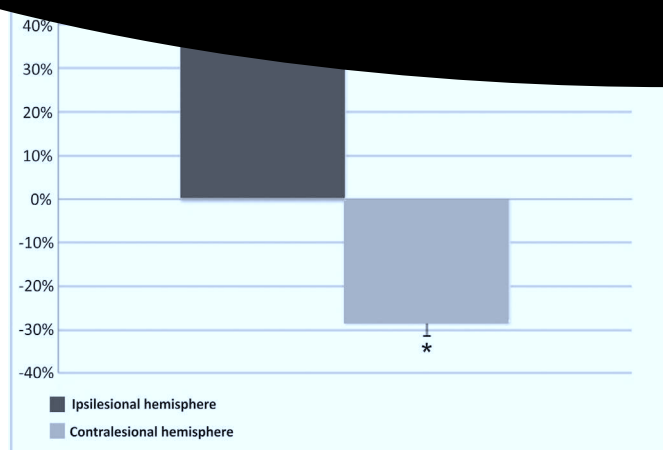


Fig. 2. Relative percent change of MEP amplitudes after iTBS applied to M1 of the affected or unaffected hemisphere compared to control stimulation. TBS applied to ipsilesional M1 induced a significant MEP increase in the stimulated hemisphere compared to control stimulation, and a significant decrease in the other (i.e., unaffected) hemisphere. Error bars: Standard error of the mean in percent (SEM).

two-sided *t*-tests ($P < 0.05$, FDR-corrected for multiple comparisons). Furthermore, coupling parameters were correlated with behavioral or electrophysiological parameters using linear correlations. In order to account for the heterogeneity of the patient sample with respect to clinical parameters, i.e., time since stroke, CST damage and lesion volumes, these factors were included as covariates in the correlation analyses.

In order to investigate whether combining parameters from fMRI, behavioral assessments and TMS yields better prediction of behavioral iTBS-aftereffects than simple Pearson correlations, we entered these variables into a linear regression model (as implemented in IBM SPSS Statistics, version 21; method: enter). The iTBS improvement score was defined as “dependent variable”. For the first model, DCM connectivity parameters showing a significant ($P < 0.05$) Pearson correlation or a statistical trend ($P < 0.1$) were defined as a block of independent variables. For the second model, the Action Research Arm Test (ARAT) score – as index of the behavioral deficit – was added as another independent variable in addition to the connectivity parameters. For the subsequent models, the different TMS parameters (resting/active/1 mV motor thresholds, SICI) were entered as additional independent variables. A model was considered significant when passing a statistical threshold of $P < 0.05$. Baseline motor performance was not correlated with iTBS aftereffects.

3. Results

3.1. Feasibility

ITBS was well tolerated by all subjects without any side effects. In one subject (P04), 1 mV MEPs could not be obtained from the ipsilesional hemisphere as the 1 mV threshold exceeded 100% stimulator output. This subject was excluded when computing iTBS-effects on MEP amplitudes, but included in all other analyses in order to maximize statistical power. Furthermore, one patient (P14) had to be excluded from the neuroimaging analysis due to excessive head movements (> 3 mm) during fMRI, but was included for assessing the iTBS-effects on MEP amplitudes.

For the two groups, neither for the ipsilesional nor for the contralateral hemisphere (independent *t*-tests; $P > 0.1$ for all comparisons). In contrast, 1 mV thresholds were significantly smaller in the patient's group compared to the healthy control group, for both the affected and the unaffected hemisphere ($P < 0.05$ for each comparison). However, there was no statistically significant difference in 1 mV thresholds between the hemispheres, neither for patients nor controls. SICI was significantly weaker in the ipsilesional hemisphere of the patient group relative to controls (patients: 0.69, controls: 0.43; $P = 0.045$; higher values denote less inhibition), while there was no difference to control subjects in SICI for the contralateral hemisphere (patients: 0.54, controls: 0.46; $P = 0.62$). Hence, stroke patients showed a reduction of inhibitory activity in the lesioned hemisphere, which is in line with earlier studies (e.g., Takechi et al., 2014).

We next tested for iTBS-effects on MEP amplitudes in chronic stroke patients. Accordingly, we performed a repeated-measure ANOVA with the factors INTERVENTION (M1-iTBS, control-iTBS) and HEMISPHERE (ipsilesional, contralateral) on percent changes in MEP amplitudes after stimulation. This analysis yielded a significant HEMISPHERE \times INTERVENTION interaction ($F_{(1,12)} = 8.70$; $P = 0.012$). *t*-tests on the relative change of MEP amplitudes showed that iTBS over ipsilesional M1 significantly increased MEPs in the stimulated, ipsilesional hemisphere compared to control stimulation (mean increase: 39%, $P = 0.032$). In contrast, MEP amplitudes in the contralateral hemisphere were significantly decreased after iTBS of ipsilesional M1 compared to control stimulation (mean decrease: -28%; $P = 0.024$) (Fig. 2). Hence, iTBS over ipsilesional M1 lead to a relative increase of excitability of the stimulated hemisphere, and a concurrent decrease of excitability of the non-stimulated hemisphere suggesting an increased transcallosal inhibition.

3.2.2. Effects of iTBS on behavioral data

We performed a repeated measure ANOVA with the factors GROUP (patients, controls) and HAND (affected, unaffected) for each of the three motor tasks (JTT, FT, GF). For each tasks, we found a significant GROUP \times HAND effect ($P < 0.005$). Post hoc *t*-tests confirmed that motor performance of the stroke-affected hand was significantly reduced for all three motor tests (JTT, FT, GF) as compared to the healthy controls ($P < 0.01$ for each comparison) while the unaffected hand was similar to that of the healthy control group.

Repeated-measures ANOVAs with the factors INTERVENTION (M1-iTBS, control-iTBS) and HAND (affected, unaffected) were computed to investigate the effect of M1-iTBS on motor performance (in percent of baseline) for each of the three motor tasks in stroke patients. None of the ANOVAs yielded a significant main effect or interaction (at least $P > 0.15$ for all comparisons). The average group effect of iTBS on motor performance in this sample of patients was, therefore, not statistically significant.

However, a more detailed analysis (Table 2) revealed that this null result on the group level could be attributed to the high interindividual variance of the responses with some patients showing improvement (e.g., up to 17.6% in JTT; P09) while others showed deterioration (e.g., up to -32.5% in JTT; P04). Here, positive values indicate an improvement after M1-iTBS as compared to control stimulation. Based on these behavioral iTBS-effects we were interested whether the behavioral susceptibility to ipsilesional M1-iTBS can even better be inferred from pre-interventional measurements using TMS and neuroimaging.

3.3. Correlation analyses

3.3.1. Correlation between TMS-parameters and M1-iTBS-effects

We first tested, whether electrophysiological TMS parameters of

P 01	13.0%			
P 02	-1.8%	-0.8%		
P 03	8.6%	-15.0%	4.6%	0.34
P 04	-32.5%	-51.6%	-29.9%	-2.52
P 05	-7.8%	-7.1%	2.0%	0.01
P 06	-22.1%	0.3%	-34.6%	-1.02
P 07	4.4%	7.9%	-0.4%	0.69
P 08	8.2%	0.0%	9.6%	0.82
P 09	17.6%	25.5%	-11.1%	1.28
P 10	-25.5%	0.0%	-4.9%	-0.48
P 11	-12.6%	-12.9%	5.6%	-0.20
P 12	-22.5%	-10.8%	-10.8%	-0.79
P 13	-2.4%	7.8%	31.0%	1.17
P 14	-2.3%	0.0%	-8.9%	0.11

Positive values = improvement after M1-iTBS as compared to control stimulation; JTT = Jebsen Taylor Hand Function test; FT = finger tapping frequency; GF = maximum grip force; Imp Score = Improvement Score (factorial analysis, 1st component).

excitability and inhibition at the M1 stimulation site indicated positive behavioral responses following ipsilesional iTBS. Correlation analyses between behavioral improvements after iTBS (improvement score) and electrophysiological TMS parameters at baseline (RMT, AMT, SICI) provided no significant results, neither for the affected nor for the unaffected hand. Likewise, we did not find significant correlations ($P > 0.1$) between iTBS-induced changes in MEP amplitudes and the TMS parameters. Hence, TMS parameters of the stimulated, ipsilesional M1 did not predict iTBS after-effects.

3.3.2. Correlation between lesion location and M1-iTBS-effects

We next computed a voxel-based lesion symptom mapping (VLSM) analysis in order to test whether lesion location was related to the iTBS aftereffect. There was a negative correlation between iTBS motor improvement score and estimated CST damage ($P < 0.05$, FDR-corrected). Plotting voxels showing significant effects revealed that especially patients with lesions of the CST at the level of paraventricular white matter were less likely to respond to iTBS (Fig. 3).

3.3.3. Correlation between fMRI activity and M1-iTBS-effects

Compared to healthy controls, stroke patients featured stronger and more widespread neural activity when moving their affected hand ($P < 0.05$, FWE-corrected at the cluster-level; Fig. 4). Overactivity was not only observed in the lesioned, but also in the contralesional (i.e., “healthy”) hemisphere. Similar results were found for both fixed and adjusted movement frequencies (Fig. 4). However, individual activity levels did not correlate with the improvement score, even at uncorrected levels, neither for the fixed nor adjusted frequency. Hence,

We next sought to investigate whether connectivity parameters may predict iTBS after-effects in chronic stroke patients.

3.4.1. Model selection

According to the random-effects Bayesian model selection, the fully connected model (model 1) showed the best model fit in both groups (exceedance probability: 99.55% in controls and 99.64% in patients) (Suppl. Fig. S3), and was used for all subsequent connectivity analyses.

3.4.2. DCM connectivity

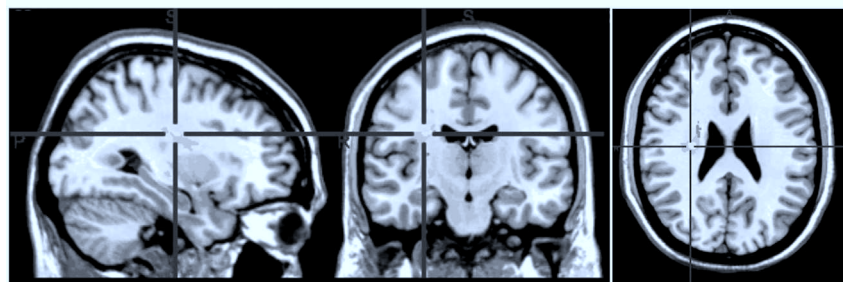
Endogenous connectivity (DCM-A) describes network interactions independent of experimental conditions, i.e., the constant or fixed part of interregional coupling for a given experimental setting. In the control group, endogenous coupling was symmetrically organized within and between hemispheres (Fig. 5A; $P < 0.05$, FDR-corrected). In the patient group, coupling strengths were generally smaller, and fewer connections became significant (Fig. 5A). Likewise, with respect to the specific effect that the movement conditions exerted on interregional coupling (DCM-B), we found weaker effects in the patients' group (Fig. 5B; $P < 0.05$, FDR-corrected). Here, especially inhibitory effects on contralesional M1 exerted by ipsilesional M1, ipsilesional SMA, and contralesional vPMC were significantly weaker in patients compared to healthy controls during movements of the affected hand (Fig. 5C; $P < 0.05$, FDR-corrected).

3.4.3. Motor network connectivity and M1-iTBS effects

To investigate whether interindividual variations in connectivity parameters predict behavioral M1-iTBS-effects, we correlated the coupling parameters with the iTBS motor improvement score. Accordingly, we found the stronger the promoting influence from ipsilesional SMA onto ipsilesional M1, and the stronger the inhibition originating from ipsilesional M1 onto contralesional M1, the more likely a patient showed improvements in hand motor function after facilitatory iTBS applied to the ipsilesional hemisphere. Both correlations were highly significant (SMA_{IL}-M1_{IL}: $r = 0.709$; M1_{IL}-M1_{CL}: $r = -0.764$; $P < 0.05$, FDR-corrected; Fig. 6). This effect remained significant when computing partial correlations, corrected for differences in time since stroke, lesion size and CST damage.

In addition, at uncorrected p -values, there was a statistical trend for higher M1-iTBS improvement scores with stronger endogenous coupling of ipsilesional vPMC onto ipsilesional M1 ($r = 0.523$; $P = 0.066$) as well as a significant effect for the influence from contralesional M1 onto ipsilesional M1 ($r = -0.557$, $P = 0.048$).

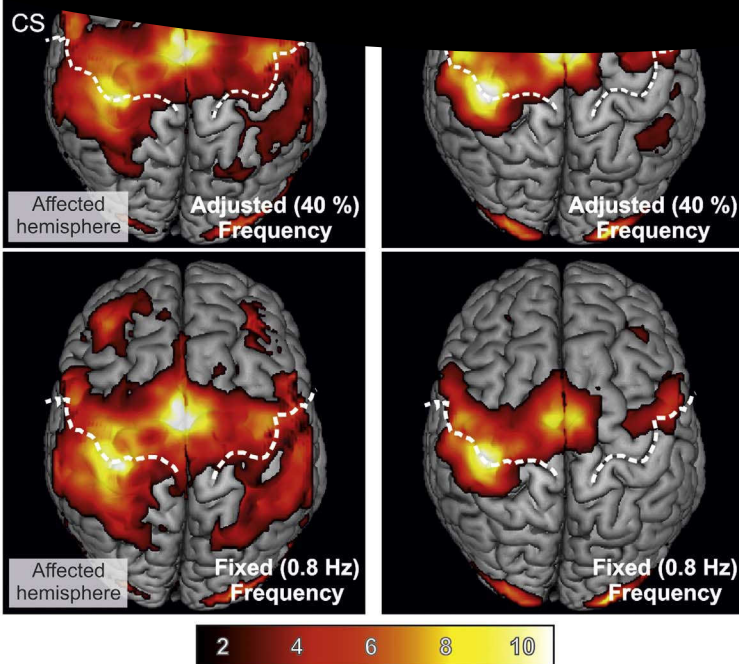
Correlation between lesions of the CST and iTBS response



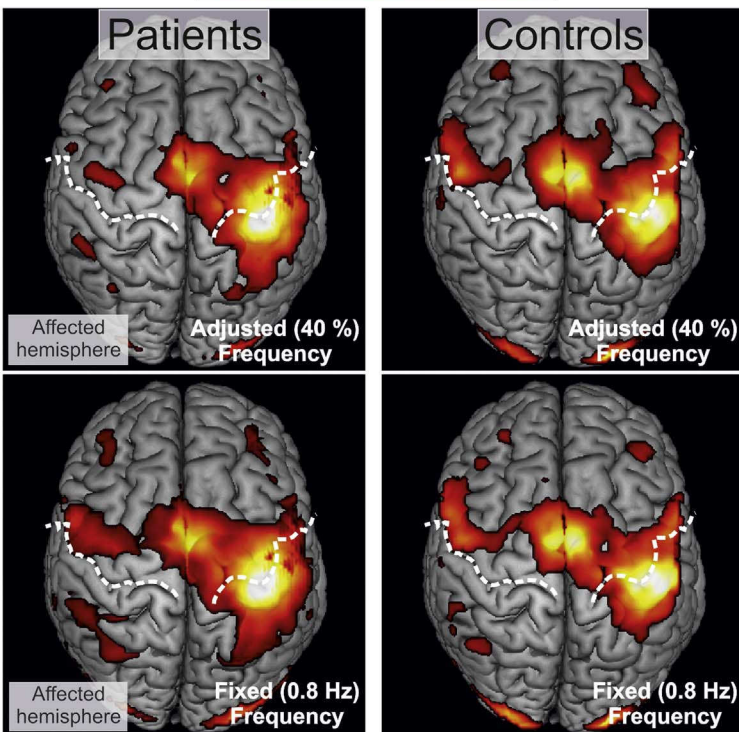
P<0.05, FDR-corrected

Fig. 3. Voxel-based lesion symptom mapping (VLSM) analysis ($P < 0.05$, FDR-corrected).

Movements Affected Hand



Movements Unaffected Hand



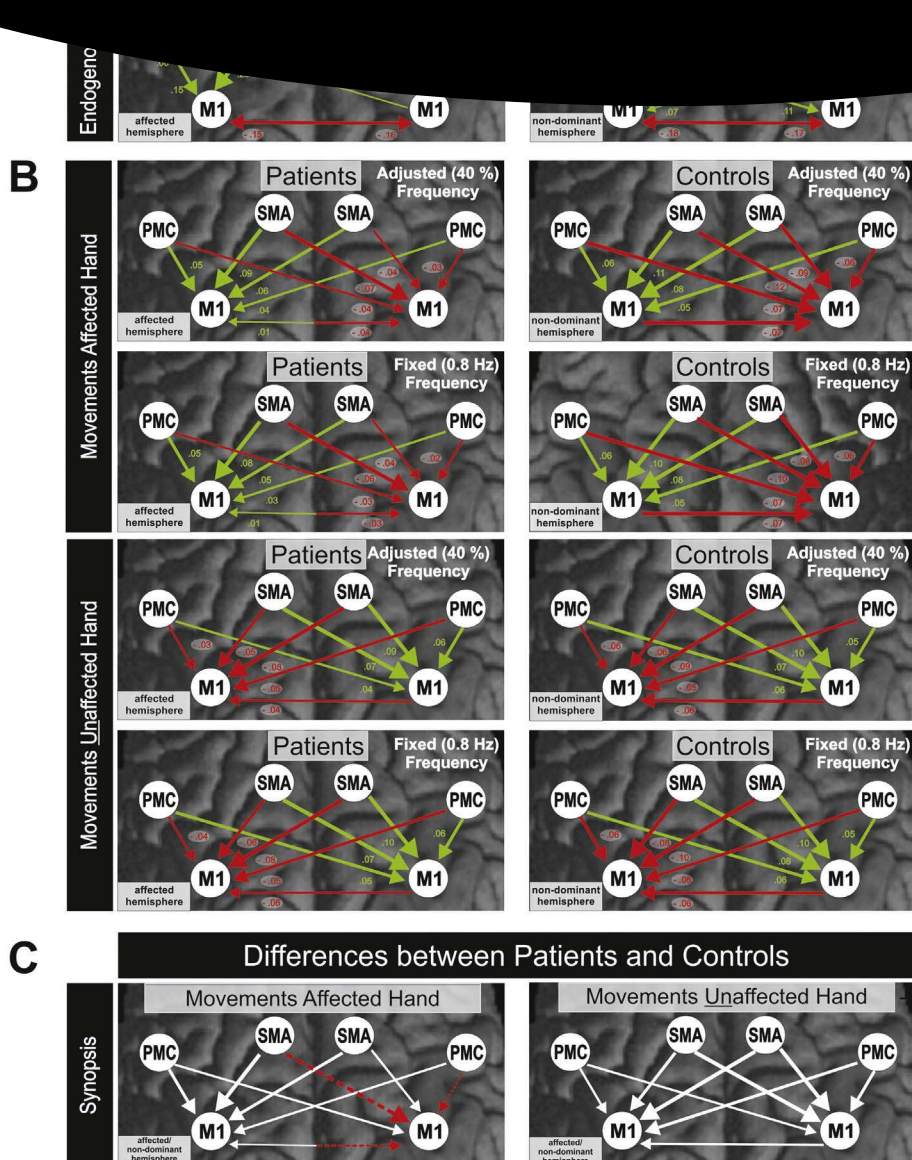
movements of the unaffected hand yielded a similar pattern in patients and controls. T-values are represented by the color bar. (For interpretation of the references to color in this figure legend, the reader is referred to the web version of this article.)

3.5. Multivariate prediction of M1-iTBS-effects

Finally, we computed linear regression models (as implemented in IBM SPSS statistics) in order to test whether combining parameters from fMRI, TMS and behavioral assessments might yield a better prediction of behavioral iTBS-aftereffects than simple Pearson correlations (variance explained: 58%).

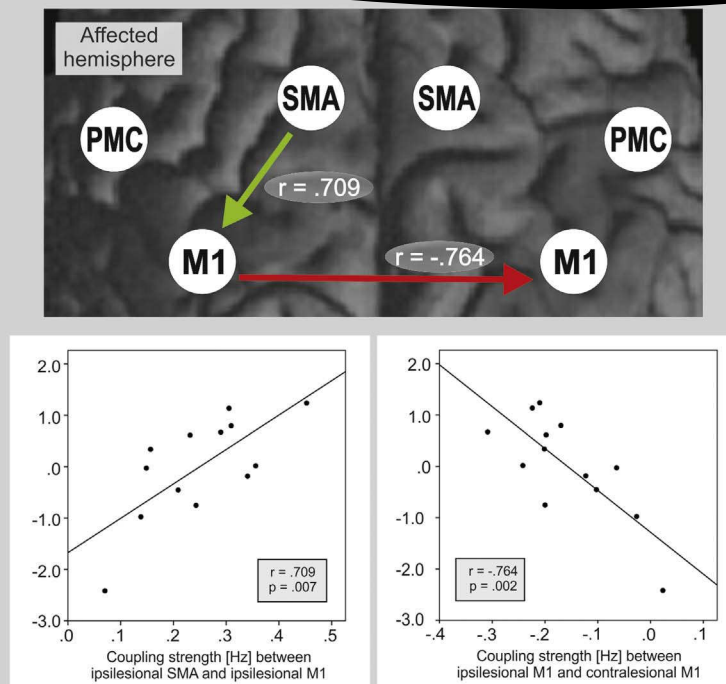
Indeed, combining the four endogenous connectivity parameters showing a significant correlation or a statistical trend with the iTBS

improvement score in a multiple regression analysis yielded a correlation coefficient of $r = 0.87$ ($r^2 = 0.76$; $F_{(4,12)} = 6.27$; $P = 0.014$). Adding the ARAT (representing the behavioral deficit) to the model increased the prediction to $r = 0.91$ ($r^2 = 0.82$; $F_{(5,12)} = 6.33$; $P = 0.016$; all betas positive except for the connection $M1_{IL}$ - $M1_{CL}$). In contrast, adding any of the TMS parameters did not further improve the model. In summary, the combination of connectivity parameters and clinical deficits assessed prior to stimulation allowed the best prediction of the behavioral M1-iTBS-aftereffects, explaining 82% of the variance.



Our data revealed that TMS parameters are poor predictors for M1-iTBS response in stroke patients. Similar conclusions have also been drawn from recent studies in healthy subjects, which also did not find a link between motor thresholds (RMT and AMT) or MEP size and M1-iTBS-aftereffects (Hamada et al., 2013; Nettekoven et al., 2015). The variability of stimulation aftereffects following rTMS interventions remains poorly understood. Animal experiments suggest that excitatory rTMS protocols like iTBS predominantly interact with certain classes of inhibitory interneurons expressing parvalbumin and calbindin (Funke and Benali, 2011; Volz et al., 2013). However, pharmacological studies with human subjects indicate that the response to iTBS at least partially depends on NMDA-receptor activity (Huang et al., 2007). Therefore, iTBS seems to interfere with various neuronal processes that might explain the complexity and variability of the stimulation aftereffects on the behavioral and electrophysiological level observed in a large

and laboratory effect of ipsilesional M1 indicated a better motor response following iTBS ($P < 0.05$, FDR-corrected).



number of rTMS/TBS studies including the present study (Di Lazzaro et al., 2011; Hamada et al., 2012; Talelli et al., 2012).

4.2. Biological variability in stroke patients

In stroke patients, further biological variance is introduced by interindividual differences in lesion size, lesion location, the amount of small-vessel disease induced white matter changes, time-since-stroke, as well as differences in medication and post-stroke treatment/rehabilitation (Adeyemo et al., 2012; Cramer, 2008). Therefore, it is well conceivable that for this population stimulation responses are even more heterogeneous than in healthy subjects. We here tried to account for these factors by using them as covariates in the statistical analyses.

While some studies reported a beneficial effect of rTMS/TBS on motor function in stroke patients (Ackerley et al., 2016; Kim et al., 2015), other studies found no measurable stimulation effects on motor performance (Malcolm et al., 2007; Talelli et al., 2012) or even deterioration of hand motor function following rTMS/TBS (Ackerley et al., 2010; Ameli et al., 2009). The present study underlines the problem of the generalizability iTBS protocol effects on changes in motor performance with some patients improving and some patients deteriorating (compared to control stimulation; cf. Table 2). However, all patients in the present study were in the chronic stage (> 12 months post-stroke). Given the fact that cellular mechanisms facilitating plasticity and reorganization are up-regulated especially in the first weeks and months after stroke (Cramer, 2008), one hypothesis is that in patients with chronic motor stroke, iTBS effects are more difficult to achieve (Hsu et al., 2012; Volz et al., 2016). Especially the combination of iTBS and motor training may further stimulate cortical plasticity and improve motor performance (Di Lazzaro et al., 2010; Wang et al., 2011). In addition to the time interval after stroke, a high degree of motor impairment and the absence of MEPs have been demonstrated to constitute negative predictors for a beneficial iTBS effect (Lai et al., 2015).

Interestingly, as the presence of MEPs depends on corticospinal tract integrity, a similar conclusion is supported by the present study, as here patients with stronger anatomical CST damage were less likely to respond to iTBS.

4.3. Neuroimaging and iTBS-effects

In line with the findings of the present study, a number of neuroimaging studies consistently demonstrated that patients with stroke-induced motor deficits show changes in motor system activity in both hemispheres during movements of the paretic hand (Grefkes et al., 2008b; Rehme et al., 2011a; Ward et al., 2003; Weiller et al., 1992). Ameli and colleagues demonstrated that patients with stronger neural activity in ipsilesional M1 show better behavioral responses to excitatory 10 Hz rTMS applied to ipsilesional M1 (Ameli et al., 2009). However, our data revealed no association between pre-interventional neural activity levels and behavioral responses stimulation with iTBS. Apart from differences in stimulation parameters, the discrepant findings might result from differences in patient populations. In the study by Ameli et al. (2009) much more patients had lesions in the motor cortex leading to reduce neural activity in this region. Most likely, in patients with larger structural deficits within the stimulation field fewer cortices can be recruited for plasticity-enhancing effects mediated by rTMS (Adeyemo et al., 2012).

4.4. Motor network connectivity and iTBS-effects

In contrast to neural activation levels, we found highly significant associations between endogenous connectivity of the stimulated M1 and behavioral effects. Our data suggested that two specific motor network characteristics allow prediction of motor improvements of the affected hand after M1-iTBS (Fig. 3): (i) pronounced promoting influences from ipsilesional SMA onto ipsilesional M1, and (ii) pronounced

lesion size, lesion location and motor impairment in terms of maximum fist closure frequency of the paretic hand that closely resembles the fMRI task used to compute the DCMs. In healthy controls, there was no relationship between motor performance (i.e., maximum fist closure frequency) and DCM coupling strength suggesting a link between motor deficits, connectivity and coupling parameters. Therefore, abnormal coupling strengths that reflect the network pathology after stroke may differ from those connections that predict the treatment response to iTBS. As outlined above, a number of studies revealed several factors in healthy subjects that are associated with a better individual response to rTMS/iTBS (Freitas et al., 2011; Hamada et al., 2012; Kleim et al., 2006). We have shown in a recent connectivity study with healthy subjects that variations in the endogenous coupling strength between premotor areas (SMA, vPMC) and M1 (i.e., the same motor areas as in the present study) predict the individual iTBS response in terms of increases in excitability within 25 min post-stimulation (Cardenas-Morales et al., 2013). Therefore, one possible conclusion is that in our sample of relatively mildly affected stroke patients the response to M1-iTBS also depends on physiological variations in motor network connectivity rather than stroke-specific changes. This hypothesis is, unfortunately, difficult to test as for obvious reasons we have no data on the pre-morbid state of connectivity in these patients. In addition, this hypothesis is challenged by findings reported in other connectivity studies which showed that neural couplings between ipsilesional SMA and M1, ipsilesional vPMC and M1 as well as between ipsilesional M1 and contralesional M1 are significantly reduced in the first days and weeks after stroke, and typically increase over time the better subjects recover (Grefkes et al., 2008b; Rehme et al., 2011a). However, the results of such an analysis would not change the primary conclusion of this study that the response to excitability-enhancing iTBS might depend on the capacity for functional integration of activity in the stimulated area within the motor network.

tion analysis results. Of note, all these effects were found in a connectivity matrix that reflects the constant part in coupling across all conditions of one experimental setting (i.e. independent from single experimental conditions). This finding suggests that intervention effects of iTBS that is applied in different sessions and even in different conditions (subjects were stimulated during rest) seem to depend on specific connections strengths rather than their task-specific modulation. These connections further correlated with behavioral impairments of patients, thereby establishing a link to disease-induced changes in corticocortical connectivity. First, they all affect M1 of the lesioned hemisphere, i.e., the motor cortex stimulated by iTBS. In addition, they match data from previous studies which showed that these connections relate to motor recovery (Rehme et al., 2011a) and - at least for the SMA-M1 connection - to stimulation aftereffects following iTBS (Cardenas-Morales et al., 2011). Furthermore, several experiments demonstrated that even simple hand movements depend on interactions within an entire network of areas rather than on M1 activity only (Grefkes et al., 2008a; Pool et al., 2013, 2014; Ward and Cohen, 2004; Witt et al., 2008). In a recent study, we investigated the interregional interactions in healthy subjects when performing fist-closures at different movement frequencies (Pool et al., 2013). These data showed that movements at higher frequencies are associated with a linear increase in neural coupling strength, especially from SMA contralateral to the moving hand onto contralateral, active M1 (Pool et al., 2013). This finding indicates that SMA contributes to variations in hand motor performance. Moreover, several studies demonstrated that TMS has affects interconnected brain regions including SMA, premotor areas and M1 (Bestmann et al., 2003; Esser et al., 2006; Grefkes et al., 2010; Hamada et al., 2009). We recently showed that in healthy subjects iTBS applied to M1 is associated with enhanced resting-state connectivity of M1 with ipsi- and contralateral premotor areas including SMA (Nettekoven et al., 2014). Therefore, it appears reasonable to conclude that behavioral effects upon M1-stimulation also depend on how effective the stimulation region is integrated into the motor system (which is exactly what DCM coupling parameters reflect) (Friston et al., 2003). It is interesting to note that also stronger inhibitory influences from ipsilesional onto contralesional M1 predicted better iTBS responses. Findings from DCM studies have shown that stronger inter-hemispheric inhibition from ipsilesional to contralesional M1 is typically found in patients with better motor recovery (Volz et al., 2015). Thus, one interpretation of this finding is that in subjects with stronger interhemispheric M1-M1 inhibition, iTBS of ipsilesional M1 might lead to a more effective suppression of the unaffected hemisphere, thereby correcting imbalances in interhemispheric competition (Hummel and Cohen, 2005). The finding that iTBS of ipsilesional M1 also effects neural processing in the contralesional hemisphere is also supported by the electrophysiological data of the present study showing a significant decrease of MEP amplitudes upon stimulation of contralesional M1 (Fig. 2). Moreover, Di Lazzaro and colleagues could demonstrate similar effects for acute stroke patients (Di Lazzaro et al., 2008).

4.5. Clinical impairment and iTBS-effects

It is a somewhat surprising result that those connections showing a significant association with iTBS-effects in stroke patients in the current study (Fig. 6) were not significantly different from those observed in healthy controls. In other words, connections that were different between patients and controls did not correlate with iTBS-aftereffects. This discrepancy might be explained by the heterogeneity of our sample of patients in terms of lesion size, CST damage and time since stroke. Our results revealed that patients with lesions of the CST (at the level of

4.6. Limitations

One point that is always discussed in studies using TMS is the control stimulation. We decided to deliver the control stimulation over the parieto-occipital vertex because a recent study reported no difference in the perception of real and sham stimulation (Herwig et al., 2010). While this stimulation has been shown to result in comparable skin sensations compared to stimulation with the center of the coil touching the skin (cf. Herwig et al., 2010), it effectively increases the coil-cortex distance, hence rendering an effective stimulation of neural tissue highly unlikely. We have used a similar setup in earlier rTMS studies and did not find any effect the control stimulation site neither on MEPs nor on fMRI connectivity (Nettekoven et al., 2014). Another limitation is that the clinical evaluator was not blinded to the stimulation condition. However, please note that the motor performance tests were highly standardized and relatively easy to perform (i.e., finger tapping recordings with a computer, grip force measurements with a vigorimeter). Further evidence that the lack of blinding of the experimenters did not have a strong impact on the can be found in the data as some patients improved and some patients deteriorated. Hence, there was no systematic bias in favor for a specific behavioral aftereffect when assessing motor performance. Importantly, the analysis of the imaging data including the connectivity analysis was completely blinded with respect to which patients improved and which not.

Furthermore, as discussed above, previous studies have already shown that rTMS interventions interfere with connectivity not only at the stimulation site but also at remote areas and that these changes correlate with behavioral improvements (Grefkes et al., 2010). However, the primary goal of the present study was to investigate whether

4.7. Conclusion

Supplementary data to this article can be found online at <http://dx.doi.org/10.1016/j.nicl.2017.06.006>.

Declaration of conflict of interests

Acknowledgements

References

- Ackerley, S.J., Stinear, C.M., Barber, P.A., Byblow, W.D., 2010. Combining theta burst stimulation with training after subcortical stroke. *Stroke* 41, 1568–1572.
- Ackerley, S.J., Byblow, W.D., Barber, P.A., MacDonald, H., McIntyre-Robinson, A., Stinear, C.M., 2016. Primed physical therapy enhances recovery of upper limb function in chronic stroke patients. *Neurorehabil. Neural Repair* 30, 339–348. <http://dx.doi.org/10.1177/1545868716654491>
- Grefkes, C., Fink, G.R., 2012. Disruption of motor network connectivity post-stroke and its noninvasive neuromodulation. *Curr. Opin. Neurol.* 25, 670–675.
- Grefkes, C., Fink, G.R., 2014. Connectivity-based approaches in stroke and recovery of function. *Lancet Neurol.* 13, 206–216.
- Grefkes, C., Eickhoff, S.B., Nowak, D.A., Dafotakis, M., Fink, G.R., 2008a. Dynamic intra-

- Grefkes, C., et al., 2013. Modulating cortical connectivity by dynamic causal modeling. *NeuroImage* 80, 100–110.
- Hamada, M., Hanajima, R., Terao, Y., Okabe, S., Nakatani-Enomoto, S., Furubayashi, T., Matsumoto, H., Shirota, Y., Ohminami, S., Ugawa, Y., 2009. Primary motor cortical metaplasticity induced by priming over the supplementary motor area. *J. Physiol.* 587, 4845–4862.
- Hamada, M., Murase, N., Hasan, A., Balaratnam, M., Rothwell, J.C., 2012. The role of interneuron networks in driving human motor cortical plasticity. *Cereb. Cortex* 23, 1593–1605.
- Hamada, M., Murase, N., Hasan, A., Balaratnam, M., Rothwell, J.C., 2013. The role of interneuron networks in driving human motor cortical plasticity. *Cereb. Cortex* 23, 1593–1605.
- Herwig, U., Fallgatter, A.J., Hoppner, J., Eschweiler, G.W., Kron, M., Hajak, G., Padberg, F., Naderi-Heiden, A., Abler, B., Eichhammer, P., Grossheinrich, N., Hay, B., Kammer, T., Langguth, B., Laske, C., Plewnia, C., Richter, M.M., Schulz, M., Unterecker, S., Zinke, A., Spitzer, M., Schonfeldt-Lecuona, C., 2007. Antidepressant effects of augmentative transcranial magnetic stimulation: randomised multicentre trial. *Br. J. Psychiatry* 191, 441–448.
- Herwig, U., Cardenas-Morales, L., Connemann, B.J., Kammer, T., Schonfeldt-Lecuona, C., 2010. Sham or real—post hoc estimation of stimulation condition in a randomized transcranial magnetic stimulation trial. *Neurosci. Lett.* 471, 30–33.
- Hoogendam, J.M., Ramakers, G.M., Di Lazzaro, V., 2010. Physiology of repetitive transcranial magnetic stimulation of the human brain. *Neuron* 45, 201–206.
- Hsu, W.Y., Cheng, C.H., Liao, K.K., Lee, I.H., Lin, Y.Y., 2012. Effects of repetitive transcranial magnetic stimulation on motor functions in patients with stroke: a meta-analysis. *Stroke* 43, 1849–1857.
- Huang, Y.Z., Edwards, M.J., Rounis, E., Bhatia, K.P., Rothwell, J.C., 2005. Theta burst stimulation of the human motor cortex. *Neuron* 45, 201–206.
- Huang, Y.Z., Chen, R.S., Rothwell, J.C., Wen, H.Y., 2007. The after-effect of human theta burst stimulation is NMDA receptor dependent. *Clin. Neurophysiol.* 118, 1028–1032.
- Huang, Y.Z., Rothwell, J.C., Lu, C.S., Wang, J., Chen, R.S., 2010. Restoration of motor inhibition through an abnormal premotor-motor connection in dystonia. *Mov. Disord.* 25, 696–703.
- Hummel, F., Cohen, L.G., 2005. Improvement of motor function with noninvasive cortical stimulation in a patient with chronic stroke. *Neurorehabil. Neural Repair* 19, 14–19.
- Hummel, F., Celnik, P., Giraux, P., Floel, A., Wu, W.H., Gerloff, C., Cohen, L.G., 2005. Effects of non-invasive cortical stimulation on skilled motor function in chronic stroke. *Brain* 128, 490–499.
- Jebens, R.H., Taylor, N., Trieschmann, R.B., Trotter, M.J., Howard, L.A., 1969. An objective and standardized test of hand function. *Arch. Phys. Med. Rehabil.* 50, 311–319.
- Khedr, E.M., Ahmed, M.A., Fathy, N., Rothwell, J.C., 2005. Therapeutic trial of repetitive transcranial magnetic stimulation after acute ischemic stroke. *Neurology* 65, 466–468.
- Kim, D.H., Shin, J.C., Jung, S., Jung, T.M., Kim, D.Y., 2015. Effects of intermittent theta burst stimulation on spasticity after stroke. *Neuroreport* 26, 561–566.
- Kleim, J.A., Chan, S., Pringle, E., Schallert, K., Procaccio, V., Jimenez, R., Cramer, S.C., 2006. BDNF val66met polymorphism is associated with modified experience-dependent plasticity in human motor cortex. *Nat. Neurosci.* 9, 735–737.
- Kolominsky-Rabas, P.L., Heuschmann, P.U., Marschall, D., Emmert, M., Baltzer, N., Neundorfer, B., Schoffski, O., Krobot, K.J., 2006. Lifetime cost of ischemic stroke in Germany: results and national projections from a population-based stroke registry: the Erlangen Stroke Project. *Stroke* 37, 1179–1183.
- Kujirai, T., Caramia, M.D., Rothwell, J.C., Day, B.L., Thompson, P.D., Ferbert, A., Wroe, S., Asselman, P., Marsden, C.D., 1993. Corticocortical inhibition in human motor cortex. *J. Physiol.* 471, 501–519.
- Lai, C.J., Wang, C.P., Tsai, P.Y., Chan, R.C., Lin, S.H., Lin, F.G., Hsieh, C.Y., 2015. Corticospinal integrity and motor impairment predict outcomes after excitatory repetitive transcranial magnetic stimulation: a preliminary study. *Arch. Phys. Med. Rehabil.* 96, 69–75.
- Luppino, G., Matelli, M., Camarda, R., Rizzolatti, G., 1993. Corticocortical connections of area F3 (SMA-proper) and area F6 (pre-SMA) in the macaque monkey. *J. Comp. Neurol.* 338, 114–140.
- Malcolm, M.P., Triggs, W.J., Light, K.E., Gonzalez Rothi, L.J., Wu, S., Reid, K., Nadeau, S.E., 2007. Repetitive transcranial magnetic stimulation as an adjunct to constraint-induced therapy: an exploratory randomized controlled trial. *Am. J. Phys. Med. Rehabil.* 86, 707–715.
- McGuire, P.K., Bates, J.F., Goldman-Rakic, P.S., 1991. Interhemispheric integration: I. Symmetry and convergence of the corticocortical connections of the left and the right principal sulcus (PS) and the left and the right supplementary motor area (SMA) in the rhesus monkey. *Cereb. Cortex* 1, 390–407.
- Mills, K.R., Boniface, S.J., Schubert, M., 1992. Magnetic brain stimulation with a double coil: the importance of coil orientation. *Electroencephalogr. Clin. Neurophysiol.* 85, 17–21.
- Muller-Dahlhaus, J.F., Orekhov, Y., Liu, Y., Ziemann, U., 2008. Interindividual variability and age-dependency of motor cortical plasticity induced by paired associative stimulation. *Exp. Brain Res.* 187, 467–475.
- Nettekoven, C., Volz, L.J., Kutscha, M., Pool, E.M., Rehme, A.K., Eickhoff, S.B., Fink, G.R., Grefkes, C., 2014. Dose-dependent effects of theta burst rTMS on cortical excitability and resting-state connectivity of the human motor system. *J. Neurosci.* 34, 68–76.
- Pool, E.M., Rehme, A.K., Fink, G.R., Eickhoff, S.B., Grefkes, C., 2013. Network dynamics and effective connectivity of the motor system. *NeuroImage* 99, 451–460.
- Quararone, A., Bagnato, S., Rizzo, V., Siebner, H.R., Dattola, V., Scalfari, A., Morgante, F., Battaglia, F., Romano, M., Girlanda, P., 2003. Abnormal associative plasticity of the human motor cortex in writer's cramp. *Brain* 126, 2586–2596.
- Rehme, A.K., Eickhoff, S.B., Wang, L.E., Fink, G.R., Grefkes, C., 2011a. Dynamic causal modeling of cortical activity from the acute to the chronic stage after stroke. *NeuroImage* 55, 1147–1158.
- Rehme, A.K., Fink, G.R., von Cramon, D.Y., Grefkes, C., 2011b. The role of the contralesional motor cortex for motor recovery in the early days after stroke assessed with longitudinal fMRI. *Cereb. Cortex* 21, 756–768.
- Rehme, A.K., Eickhoff, S.B., Rottschy, C., Fink, G.R., Grefkes, C., 2012. Activation likelihood estimation meta-analysis of motor-related neural activity after stroke. *NeuroImage* 59, 2771–2782.
- Rehme, A.K., Eickhoff, S.B., Grefkes, C., 2013. State-dependent differences between functional and effective connectivity of the human cortical motor system. *NeuroImage* 67, 237–246.
- Rehme, A.K., Volz, L.J., Feis, D.L., Eickhoff, S.B., Fink, G.R., Grefkes, C., 2015. Individual prediction of chronic motor outcome in the acute post-stroke stage: behavioral parameters versus functional imaging. *Hum. Brain Mapp.* 36, 4553–4565.
- Ridding, M.C., Rothwell, J.C., 2007. Is there a future for therapeutic use of transcranial magnetic stimulation? *Nat. Rev. Neurosci.* 8, 559–567.
- Rizzolatti, G., Luppino, G., 2001. The cortical motor system. *Neuron* 31, 889–901.
- Rossini, P.M., Barker, A.T., Berardelli, A., Caramia, M.D., Caruso, G., Cracco, R.Q., Dimitrijevic, M.R., Hallett, M., Katayama, Y., Lucking, C.H., et al., 1994. Non-invasive electrical and magnetic stimulation of the brain, spinal cord and roots: basic principles and procedures for routine clinical application. Report of an IFCN committee. *Electroencephalogr. Clin. Neurophysiol.* 91, 79–92.
- Rouiller, E.M., Babalian, A., Kazennikov, O., Moret, V., Yu, X.H., Wiesendanger, M., 1994. Transcallosal connections of the distal forelimb representations of the primary and supplementary motor cortical areas in macaque monkeys. *Exp. Brain Res.* 102, 227–243.
- Stephan, K.E., Penny, W.D., Daunizeau, J., Moran, R.J., Friston, K.J., 2009. Bayesian model selection for group studies. *NeuroImage* 46, 1004–1017.
- Stinear, C.M., Barber, P.A., Petoe, M., Anwar, S., Byblow, W.D., 2012. The PREP algorithm predicts potential for upper limb recovery after stroke. *Brain* 135, 2527–2535.
- Takechi, U., Matsunaga, K., Nakanishi, R., Yamanaga, H., Murayama, N., Mafune, K., Tsuji, S., 2014. Longitudinal changes of motor cortical excitability and transcallosal inhibition after subcortical stroke. *Clin. Neurophysiol.* 125, 2055–2069.
- Talelli, P., Cheeran, B.J., Teo, J.T., Rothwell, J.C., 2007a. Pattern-specific role of the current orientation used to deliver theta burst stimulation. *Clin. Neurophysiol.* 118, 1815–1823.
- Talelli, P., Greenwood, R.J., Rothwell, J.C., 2007b. Exploring theta burst stimulation as an intervention to improve motor recovery in chronic stroke. *Clin. Neurophysiol.* 118, 333–342.
- Talelli, P., Wallace, A., Dileone, M., Hoad, D., Cheeran, B., Oliver, R., VandenBos, M., Hammerbeck, U., Barratt, K., Gillini, C., Musumeci, G., Boudrias, M.H., Cloud, G.C., Ball, J., Marsden, J.F., Ward, N.S., Di Lazzaro, V., Greenwood, R.G., Rothwell, J.C., 2012. Theta burst stimulation in the rehabilitation of the upper limb: a semi-randomized, placebo-controlled trial in chronic stroke patients. *Neurorehabil. Neural Repair* 26, 976–987.
- Volz, L.J., Benali, A., Mix, A., Neubacher, U., Funke, K., 2013. Dose-dependence of changes in cortical protein expression induced with repeated transcranial magnetic theta-burst stimulation in the rat. *Brain Stimul.* 6, 598–606.
- Volz, L.J., Rehme, A.K., Michely, J., Nettekoven, C., Eickhoff, S.B., Fink, G.R., Grefkes, C., 2016. Shaping Early Reorganization of Neural Networks Promotes Motor Function after Stroke. *Cereb. Cortex* 26, 2882–2894.
- Volz, L.J., Sarfeld, A.S., Diekhoff, S., Rehme, A.K., Pool, E.M., Eickhoff, S.B., Fink, G.R., Grefkes, C., 2015. Motor cortex excitability and connectivity in chronic stroke: a multimodal model of functional reorganization. *Brain Struct. Funct.* 220, 1093–1107.
- Wang, L.E., Fink, G.R., Diekhoff, S., Rehme, A.K., Eickhoff, S.B., Grefkes, C., 2011. Noradrenergic enhancement improves motor network connectivity in stroke patients. *Ann. Neurol.* 69, 375–388.
- Ward, N.S., Cohen, L.G., 2004. Mechanisms underlying recovery of motor function after stroke. *Arch. Neurol.* 61, 1844–1848.
- Ward, N.S., Brown, M.M., Thompson, A.J., Frackowiak, R.S., 2003. Neural correlates of motor recovery after stroke: a longitudinal fMRI study. *Brain* 126, 2476–2496.
- Wassermann, E.M., 1998. Risk and safety of repetitive transcranial magnetic stimulation: report and suggested guidelines from the International Workshop on the Safety of Repetitive Transcranial Magnetic Stimulation, June 5–7, 1996. *Electroencephalogr. Clin. Neurophysiol.* 108, 1–16.
- Weiller, C., Chollet, F., Friston, K.J., Wise, R.J., Frackowiak, R.S., 1992. Functional reorganization of the brain in recovery from striatocapsular infarction in man. *Ann. Neurol.* 31, 463–472.
- Witt, S.T., Laird, A.R., Meyerand, M.E., 2008. Functional neuroimaging correlates of finger-tapping task variations: an ALE meta-analysis. *NeuroImage* 42, 343–356.
- Ziemann, U., 2004. TMS and drugs. *Clin. Neurophysiol.* 115, 1717–1729.